Chapter 1
Anion Exchange Resin Modified with Nanoparticles of Hydrated Zirconium Dioxide for Sorption of Soluble U(VI) Compounds

Olga Perlova, Yuliya Dzyazko, Iryna Halutska, Nataliia Perlova, and Alexey Palchik

1.1 Sorption Materials for Removal of Soluble U(VI) Compounds from Water

Besides military industry, uranium is also applied to civilian needs. Uranium compounds are employed in geology (to determine age of rocks), as a pigment for paints, in analytical chemistry, and for other purposes [1]. However, produced uranium is mainly consumed by nuclear power plants. Therefore, mining and processing of uranium ores are important practical tasks. Efficient, accessible, and cheap methods for the removal of U(VI) compounds from liquid wastes could provide ecological hygiene in uranium extraction from mineral raw materials. Moreover, the technique has to cover uranium recuperation in order to prevent appearance of toxic ions in sources of water supply. Adsorption and ion exchange present a possibility to decrease the content of U(VI) compounds down to maximum allowable concentration [2]. The following characteristics for materials are required: significant capacity and selectivity toward uranium-containing ions, high sorption rate, and facile regeneration. Currently, attention is focused on change of chemical composition of organic (particularly biopolymers) or inorganic sorbents. This is achieved by treatment of the materials with solutions of metal chlorides (Li^+, Na^+, K^+, Mg^{2+}, Ca^{2+}, Fe^{2+}, and Zn^{2+}) [3], acids [3–5] or alkali [4–6] (sometimes simultaneously with irradiation [6]). Natural or synthetic materials are also modified with functional groups, which are able to form complexes with sorbed ions [7]. For example, silica is functionalized with phosphate groups [8]; graphene oxide is modified with phenanthroline diamide [9]. The other way

O. Perlova · I. Halutska · N. Perlova (✉)
Odessa I.I. Mechnikov National University, Odesa, Ukraine

Y. Dzyazko · A. Palchik
V.I. Vernadskii Institute of General and Inorganic Chemistry of the National Academy of Sciences of Ukraine, Kyiv, Ukraine

O. Fesenko, L. Yatsenko (eds.), *Nanooptics, Nanophotonics, Nanostructures, and Their Applications*, Springer Proceedings in Physics 210,
https://doi.org/10.1007/978-3-319-91083-3_1

is the development of composites, particularly organic–inorganic sorbents. Combination of constituents of different nature allows us to obtain materials that possess improved functional properties compared to individual components. Different substances are applied to synthesize the composites. These materials contain, for instance, iron nanoparticles [10, 11], Fe_3O_4 [12–18] (particularly functionalized with organic functional groups [18]), MgO [19], ZrO_2 [20, 21], layered double oxides of multivalent metals [22, 23], and functionalized polymers, such as polyacrylonitrile [24] (amidoxime has been proposed for its functionalization [13, 25–28]). Other composites are considered in [28–33]. The polymer constituents are poly(vinyl imidazole) [28], polyaniline [29, 30], tetraphenylmethylenediphospine dioxide [31], and poly(vinyl alcohol) [32, 33]. The polymers are modified with molybdenum disulfide [28], mesoporous carbon [29], oxidized graphene [30], carbon nanotubes [32], or silica [33].

Among polymer matrices, ion exchange resins are the most attractive materials due to their availability, low cost, significant sorption capacity, and high rate of sorption. In order to improve selectivity toward uranium, the resins are modified with inorganic ion-exchangers [34–38], organic compounds [39–43], or microorganisms [44]. However, the modified resins show lower sorption rate than pristine materials. The composites containing non-aggregated nanoparticles show higher rate of sorption of transition metal ions [38, 45] than the resin modified with large particles (aggregates and agglomerates) [37, 46]. Approaches based on the Ostwald–Freundlich equation have been proposed in order to control the size of particles in inert [47] and cation exchange polymers [38, 48]. In the last case, the equation has been adopted taking properties of the matrix into consideration.

As known, sodium carbonate and sulfuric acid are applied to uranium ore processing [1]. Anionic forms of U(VI) dominate in carbonate and sulfate solutions [49]. It is the same also for groundwater, which normally contains carbonate anionic complexes. The aim of the investigation was to develop an approach for purposeful control of the size of the particles incorporated into anion exchange polymer. The tasks of the work were to confirm the approach experimentally and to study sorption of uranium-containing anions.

1.2 Synthesis of Composite Sorbents. A Study of Their Morphology

EDE-10P anion exchange resin (Schekinoazot, RF) was used as the polymer matrix for modification. The pristine resin was marked AR-0. This material contains such functional groups as $-NR_3^+$, =NH, and $-NR_2$. Particles of hydrated zirconium dioxide (HZD) were precipitated in the matrix. This amphoteric inorganic ion-exchanger is characterized by anion exchange ability in neutral and acidic media [50, 51]. Under these conditions, HZD (particularly in combination with oxide of other multivalent metals [52]) shows considerable capacity and rather fast rate of sorption of anionic forms of transition metals ($HCrO_4^-$ [51, 52]) and even

cations (Cu^{2+}, Cd^{2+}, Pb^{2+} [52]). Due to these remarkable properties, HZD is used for modification of ceramic [53–56] or polymer membranes [47, 57, 58]. Modified membranes based on inert polymers show higher rejection of colloidal particles than the pristine materials [47, 57]. HZD slows down transport of co-ions through polymer anion exchange membranes [58]. Moreover, the incorporated particles prevent fouling of the membranes with organics. HZD was also applied to modification of both cation [59] and anion [60] exchange resins. Modification improves selectivity of the ion-exchangers toward transition metal cations [59] and arsenate anions [60].

The ion-exchanger was impregnated with a 0.1 M $ZrOCl_2$ aqueous solution during 24 h at 25 °C. The ratio of volumes of solid and liquid was 1:20. Then the ion-exchanger and solution were separated and the grains were washed with a 0.01 M HCl to remove additionally sorbed electrolyte from macropores. The inorganic constituent was precipitated with a 1 M NH_4OH solution. The AR-1 sample was obtained in this manner.

In order to obtain the AR-2 ion-exchanger, similar modification procedure was applied. However, both impregnation and precipitation were carried out at 100 °C.

Concentration of $ZrOCl_2$ and NH_4OH solutions was 1 M, when the AR-3 and AR-4 samples were synthesized. The temperature of impregnating and precipitating solutions was kept at the level of 25 °C (AR-3) and 100 °C (AR-4).

For synthesis of the AR-5 sample, a mixture of water (20 vol %) and glycerol (80 vol %) was used for preparation of 0.1 M $ZrOCl_2$ and 0.1 M NH_4OH solutions. The water–glycerol mixture was also used for washing of the resin loaded with $ZrOCl_2$. The synthesis temperature was 25 °C.

After precipitation, the samples were washed with deionized water down to constant pH of the effluent, washed at room temperature down to constant mass, and treated with ultrasound at 30 kHz using a Bandelin ultrasonic bath (Bandelin, Hungary). This treatment was necessary to remove inorganic particles from outer surface of the grains.

TEM images were obtained with a JEOL JEM 1230 transmission electron microscope (JEOL, Japan). Preliminarily, the ion-exchangers were milled and treated with ultrasound.

1.3 Investigation of U(VI) Sorption and Desorption

Salts of uranyl acetate and sodium hydrocarbonate (Chemapol, Czech Republic) were used for preparation of modeling solutions containing 2×10^{-4} M U(VI). Anionic complexes of uranyl ($[UO_2(CO_3)]_2^{2-}$) dominated in the solution that contained also 0.02 M $NaHCO_3$ (pH 7).

Sorption was investigated under batch conditions at 20 °C. A Water Bath Shaker type 357 apparatus (Elpan, Poland) was used for shaking of the flasks during 15–180 min. The volume of the solution was 50 cm^3. The sorbent dosage is pointed for each particular case (mass of air-dry sorbent was taken into consideration).

Preliminarily, the samples were treated with deionized water for swelling. During the contact of solid and liquid, the pH was controlled with an I–160 MI pH-meter (Izmeritelnaya technika LTD, RF).

After predetermined time, the liquid was separated from the ion-exchanger, uranium(VI) in the solution was determined in the form of complex with Arsenazo III [61] using KFK-2MP photocolorimeter (Zagorsk OMZ, RF). Removal degree of uranium (*RD*) was determined as $\frac{C_0-C}{C_0} \times 100\%$, where C_0 and C are concentrations of the solution before and after sorption. Sorption capacity (A) was calculated via $\frac{V\ (C_0-C)}{m}$, where V is the solution volume, m is the mass of weighted sample.

The *RD* and A values that correspond to equilibrium conditions were also determined. These samples, which were loaded with U(VI) as fully as possible (the sorbent dosage was 1 g dm^{-3}, the solution volume was 50 cm^3), were regenerated. Preliminarily, the resins were dried at room temperature down to constant mass. Desorption was carried out under batch conditions, the content of the flasks was stirred intensively as mentioned earlier. Deionized water or 1 M one-component solutions of NaOH or $NaHCO_3$ were used for regeneration, their volume was 50 cm^3. Regeneration with an $NaHCO_3$ solution was performed two times. Desorption was carried out during 2 h. Then the solid and liquid were separated, the content of U(VI) in the effluent was determined. Desorption degree (*DD*) was calculated as $\frac{C_d}{C_0-C} \times 100\%$, where C_d is the content of uranium in the effluent.

1.4 Precipitation of HZD in Anion Exchange Polymer: Theory

Let us consider precipitation of hydrated oxide (we will write down its formula as $Cat(OH)_z$ for simplicity) inside anion-exchange resin. During precipitation, dissolution of small particles and their reprecipitation on larger particles occur. Decrease of the particle surface causes reduction of Gibbs energy. In this case, the Ostwald–Freundlich equation [62] is valid:

$$\ln \frac{\bar{C}_{Cat(OH)_z}}{C_{Cat(OH)_z,\infty}} = \frac{\beta V_m \sigma \mathrm{Cos}\,\phi}{\mathrm{RTr}}. \tag{1.1}$$

Here $\bar{C}_{Cat(OH)_z}$ and $C_{Cat(OH)_z,\infty}$ are the concentrations of dissolved compound in ion-exchanger and saturated solution, respectively (regarding insoluble compounds, these values are extremely low), β is the shape factor of particles, V_m is the molar volume of the compound, σ is the surface tension of the solvent, ϕ is the wetting angle ($\approx$1 for hydrophilic compound), and r is the particle radius.

Thus, $\bar{C}_{\mathrm{Cat(OH)}_z} = \left[\overline{\mathrm{Cat}}^{z+}\right] = \dfrac{K_{sp}}{[\mathrm{OH}]^z}$, here the square brackets correspond to equilibrium molar concentration, K_{sp} is the solubility product, z is the charge number. Dissociation degree of NH_4OH (α) can be determined according to Ostwald dilution law [63]:

$$\alpha = K^{0.5}_{\mathrm{NH_4OH}} C^{0.5}_{\mathrm{NH_4OH}} \tag{1.2}$$

where K_{NH_4OH} is the dissociation constant of NH_4OH, C_{NH_4OH} means concentration. The precipitating solution provides certain equilibrium concentration of OH^- ions.

$$[\mathrm{OH}^-] = [\mathrm{NH_4}] = \alpha \mathrm{C}_{\mathrm{NH_4OH}} \tag{1.3}$$

Taking formula (1.2) into consideration, Eq. (1.3) can be written as

$$[\mathrm{OH}^-] = K^{0.5}_{\mathrm{NH_4OH}} C^{1.5}_{\mathrm{NH_4OH}} \tag{1.4}$$

OH^- ions are partially consumed for $Cat(OH)_z$ deposition:

$$\mathrm{Cat}^{z+} + z\mathrm{OH}^- \leftrightarrow \mathrm{Cat(OH)}_z \downarrow \tag{1.5}$$

This consumption is equal to zC_{Cat}. In the first approximation, it is possible to suppose that the volume of additionally sorbed electrolyte (zirconium hydroxocomplexes in our case) corresponds to the volume of the ion-exchanger (V_i). Resulting concentration of OH^- ions is

$$[\mathrm{OH}^-] = K^{0.5}_{\mathrm{NH_4OH}} C^{1.5}_{\mathrm{NH_4OH}} - \frac{zC_{\mathrm{Cat}} V_i}{V_{\mathrm{NH_4OH}}}, \tag{1.6}$$

where V_{NH_4OH} is the volume of the precipitating solution. Thus,

$$\bar{C}_{\mathrm{Cat(OH)}_z} = \frac{K_{sp}}{\left(K^{0.5}_{\mathrm{NH_4OH}} C^{1.5}_{\mathrm{NH_4OH}} - \frac{zC_{\mathrm{Cat}} V_i}{V_{\mathrm{NH_4OH}}}\right)^z} \tag{1.7}$$

Substituting this expression into Eq. (1.1), it is possible to obtain

$$r = \frac{\beta V_m \sigma}{RT \ln \dfrac{K_{sp}}{C_{\mathrm{Cat(OH)}_z,\infty}\left(K^{0.5}_{\mathrm{NH_4OH}} C^{1.5}_{\mathrm{NH_4OH}} - \frac{zC_{\mathrm{Cat}} V_i}{V_{\mathrm{NH_4OH}}}\right)^z}} \tag{1.8}$$

The particles, the size of which is lower than the r value, are dissolved and reprecipitated as larger particles. In accordance with expression (1.8), increase in temperature provides formation of smaller particles. Decrease in concentration of precipitant and additionally sorbed electrolyte as well as reducing of surface tension of solvent give the same results.

1.5 Visualization of Incorporated Particles

As seen from the TEM images (Fig. 1.1), the AR-1 sample contains single nanoparticles, the size of which is about 5 nm and even smaller. Some nanoparticles are placed close to each other, but they are isolated. HZD nanoparticles are evidently located in nanosized pores (clusters and channels), similarly to nanoparticles of zirconium hydrophosphate embedded to cation exchange resin [38, 64]. The nanoparticles are stabilized by pore walls.

Large particles (≈200–300 nm) have been found for the AR-2 sample. Their shape is close to globular. It is seen that the particles consist of smaller nanoparticles (≈30 nm). These aggregates can be located in hydrophobic pores of the ion exchange polymer (voids between gel regions). As opposed to Eq. (1.8), increase in synthesis temperature results in enlargement of the particles. Aggregation is probably caused by thermal motion of polymer chains. As a result, pore walls cannot perform stabilization function under these conditions. From the point of view of thermodynamics, enlargement of HZD particles can be caused by increase of the $C_{\mathrm{Cat(OH)}_z,\infty}$ and $K_{\mathrm{NH_4OH}}$ values.

Increase in concentration of the impregnating solution leads to enlargement of HZD particles as opposed to Eq. (1.8). However, hydrolysis of zirconium-containing ions becomes stronger when the impregnating solution is diluted. When $ZrOCl_2$ salt is dissolved in aqueous media, zirconium ions form soluble polymerized hydroxocomplexes. Among the ligands (OH^- and H_2O), water molecules

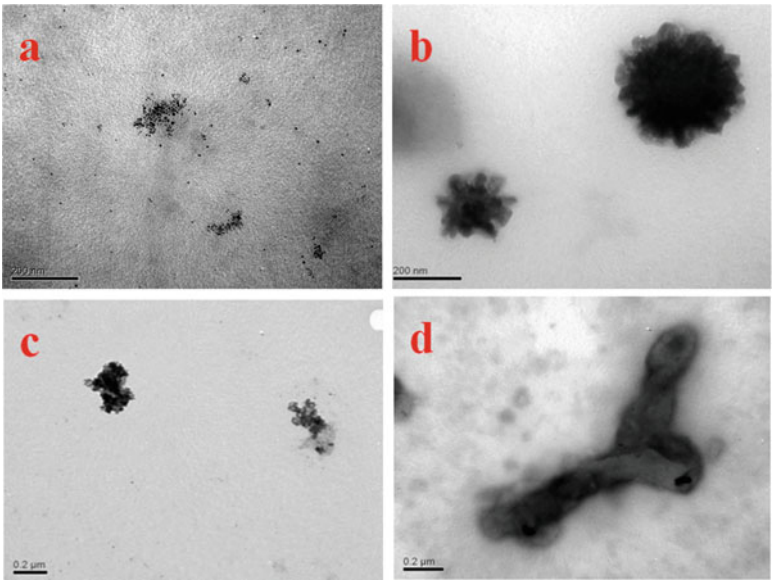

Fig. 1.1 TEM images of AR-1 (**a**), AR-2 (**b**), AR-3 (**c**), and AR-5 (**d**) samples

dominate [65]. Dilution of the solution enhances hydrolysis. As a result, the amount of OH^- ligands around zirconium atoms increases; they replace water molecules. It means reducing of molar volume of HZD and decrease of particle size in accordance with Eq. (1.8). The data obtained for the AR-4 samples are similar to those for the AR-2 resin.

According to Eq. (1.8), decrease of surface tension reduces particle size ($\sigma = 59.4$ and 72.8 mN m^{-1} at 20 °C for glycerol and water, respectively). However, large aggregated particles of irregular shape are formed in the glycerol–water mixture (AR-5). These particles are of micron size and can be located in structure defects. Molar volume of the precipitant becomes larger when it is deposited from glycerol-containing solution due to formation of insoluble Zr complexes containing both glycerol and OH ligands. Indeed, both dark and light spots are visible in TEM image. Dark spots correspond to regions where water dominates. Lights spots are attributed to regions where glycerol dominates in HZD.

1.6 Uranium Sorption Under Batch Conditions

Removal degree of U(VI) from modeling solutions is plotted in Fig. 1.2a, b for all tested samples (sorbent dosage was 1 g dm^{-3}). It has been found for all composites (except AR-5) that incorporated nanoparticles accelerate sorption. Both the pristine resin and composites containing particle, the size of which is from several nanometers up to several hundred nanometers, show practically complete removal of U(VI) from the solutions after 150–250 min. In the case of the AR-5 sample, RD = 85% after 250 min. The most complete removal is reached only after 1400 min. It is seen from Fig. 1.2c that the sorption rate strongly depends on dosage of the sorbent. Increase of the sorbent amount in the solution accelerates sorption.

The models of film and particle diffusion [66], chemical reactions of the pseudo-first [67] and pseudo-second order [68] were applied to experimental data. As found, the AR-0, AR-2, and AR-4 composites obey the model of the pseudo-first order:

$$\ln (A_\infty - A_t) = \ln A_\infty - K_1 t. \tag{1.9}$$

At the same time, the model of the pseudo-second order:

$$\frac{t}{A} = \frac{1}{K_2 A_\infty^2} + \frac{1}{A_\infty} \cdot t \tag{1.10}$$

is applied to other samples. Here A_t and A_∞ are the capacity after certain time and under equilibrium conditions, respectively, K_1 and K_2 are the constants. The calculated data are given in Fig. 1.3 and summarized in Tables 1.1 and 1.2. The experimental and calculated A_∞ values are rather close to each other. This and also high correlation coefficients show adequacy of the models.

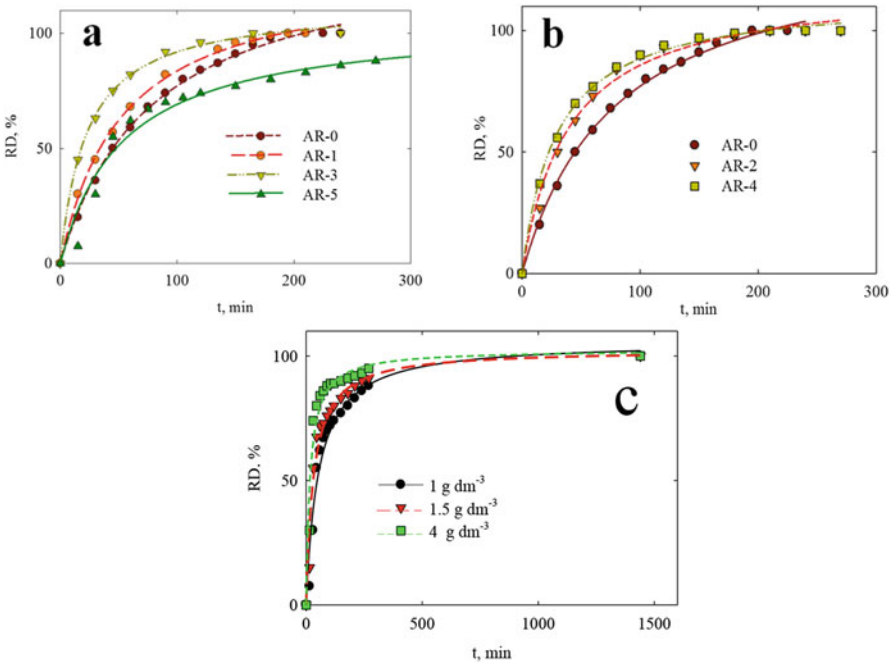

Fig. 1.2 Removal degree of uranium(VI) from modeling solution over time. Sorbent dosage was 1 g dm^{-3} (**a**, **b**, all samples) or varied (**c**. AR-5)

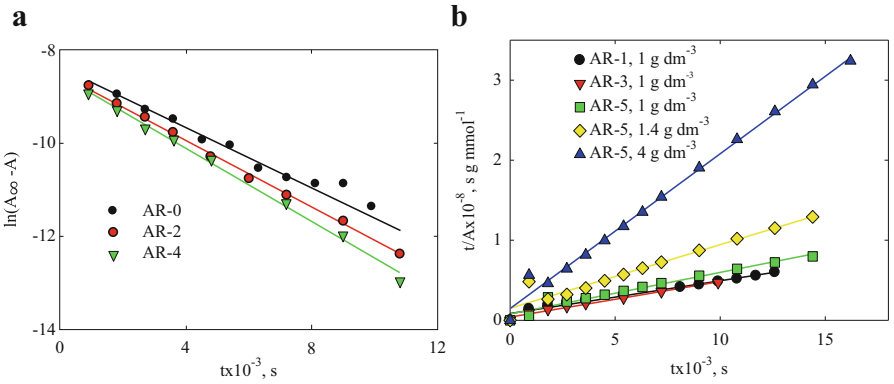

Fig. 1.3 Application of the model of chemical reaction of pseudo-first (**a**) and pseudo-second order (**b**). The sorbent dosage was 1 g dm^{-3} (**a**) or varied as the legend shows (**b**)

The highest constant for the chemical reaction of the pseudo-first order has been found for the AR-4 sample. It is 1.3 times higher than that for the pristine resin. Regarding the K_2 magnitudes, the AR-3 sample shows the highest constant (among the data for sorbent dosage of 1 g dm^{-3}). It should be stressed that the sorbents,

Table 1.1 Uranium(VI) sorption: model of chemical reaction of pseudo-first order

Sample	$A_\infty \times 10^4$, mol g^{-1}		$K_1 \times 10^4$, s^{-1}	R^2
	Experimental	Calculated		
AR-0	2.11	2.02	2.92	0.98
AR-2	1.05	1.01	3.64	0.99
AR-4	1.05	1.01	3.73	0.99

Table 1.2 Uranium(VI) sorption: model of chemical reaction of pseudo-second order

Sample	Dosage, g dm^{-3}	$A_\infty \times 10^4$, mol g^{-1}		K_2, g mol^{-1} s^{-1}	R^2
		Experimental	Calculated		
AR-1	1.0	2.10	2.66	1.19	0.99
AR-3	1.0	2.10	2.41	2.92	0.99
AR-5	1.0	2.10	2.21	1.19	0.99
	1.5	1.24	1.28	3.61	0.99
	4.0	0.52	0.53	18.5	0.99

which were obtained using more concentrated $ZrOCl_2$ solution, demonstrate the highest sorption rate. These samples contain mainly aggregated nanoparticles, the size of which is several hundred nanometers. At the same time, the lowest K_2 value has been found for the sample containing particles of micron size (AR-5). Sorption can be accelerated only by means of increasing the sorbent dosage.

1.7 Regeneration of Sorbents

Certain samples loaded with U(VI) were regenerated with different reagents (Table 1.3). No sufficient uranium removal from the resins was observed during their treatment with deionized water. However, treatment with NaOH solution allows us to reach rather high desorption degrees (41–62%). The lowest desorption degree has been found for the AR-1 sample, which contains non-aggregated nanoparticles. The pristine resin demonstrates the highest *DD* value. The most complete regeneration is achieved when $NaHCO_3$ solution is used. After double washing with this solution, the *DD* magnitude is 100% (AR-1) or close to it (other composites). In this case, ion exchange is enhanced by complex formation. The *DD* values decreases in the following order: AR-1 > AR-3 > AR-5. A size of incorporated particles reduces as follows: AR-5 > AR-3 > AR-1. It means the most facile regeneration is characteristic for the ion-exchangers containing non-aggregated nanoparticles. The lowest desorption degree is reached for the pristine resin.

In order to use the sorbents further, their hydrocarbonate forms have to be transformed into OH-forms by means of washing with alkali solution. This is necessary to provide high sorption rate.

Table 1.3 Regeneration of sorbents

Reagent	*DD*, %			
	AR-0	AR-1	AR-3	AR-5
H_2O	1	2	4	3
NaOH	62	41	61	53
$NaHCO_3$ (1 time)	66	95	83	84
$NaHCO_3$ (2 times)	89	100	98	95

1.8 Conclusions

The Ostwald–Freundlich equation was adapted to HZD precipitation in anion exchange polymer matrix. Experimental verification shows that the chemical composition of incorporated particles has to be taken into consideration. Non-aggregated nanoparticles can be obtained at room temperature and concentration of impregnating solution of 0.1 M. Increase of concentration of $ZrOCl_2$ solution and elevation of temperature provide formation of particles, the size of which is several hundred nanometers. Depending on type of incorporated particles, the rate of sorption of uranium-containing anions obeys the model of chemical reaction of pseudo-first or pseudo-second order. Among other tested sorbents, the samples that contain particles in voids between gel regions show the highest sorption rate.

Insertion of glycerol to the solvent provides precipitation of large particles of micron size. This sample demonstrates the slowest sorption rate; it is lower in comparison even with the pristine resin.

As found, the most suitable reagent for regeneration is $NaHCO_3$ solution. Decrease in size of incorporated particles has been established to facilitate desorption of uranium-containing anions.

References

1. Morrell JS, Jackson MJ (eds) (2013) Uranium processing and properties. Springer Science + Business Media, New York
2. WHO (2008) Guidelines for drinking-water quality, 3rd ed. Incorporating the first and second addenda, vol 1. Recommendations. Geneva
3. Shakur HR, Saraee KRE, Abdi MR et al (2016) Selective removal of uranium ions from contaminated waters using modified-X nanozeolite. Appl Radiat Isot 118:43–55
4. Yakout SM (2016) Evaluation of mineral and organic acids on the selective separation of radioactive elements (U and Th) using modified carbon. Desalin Water Treat 57(7):3292–3297
5. Yi ZJ, Yao J, Kuang YF et al (2016) Uptake of hexavalent uranium from aqueous solutions by using coconut husk activated carbon. Desalin Water Treat 57(4):1749–1755
6. Menacer S, Lounis A, Guedioura B et al (2016) Uranium removal from aqueous solutions by adsorption on Aleppo pine sawdust, modified by NaOH and neutron irradiation. Desalin Water Treat 57(34):16184–16195
7. Loureiro JM, Kartel MT (eds) (2009) Combined and hybrid adsorbents: fundamentals and applications. Springer, Berlin

8. Das A, Sundararajan M, Paul B et al (2017) Assesment of Phosphate Functionalised Silica Gel (PFSG) for separation and recovery of uranium from Simulated Silicide Fuel Scraps Dissolver Solution (SSFSDS). Colloids Surf A Physicochem Eng Asp 530:124–133
9. Li F, Yang Z, Weng H et al (2018) High efficient separation of U(VI) and Th(IV) from rare earth elements in strong acidic solution by selective sorption on phenanthroline diamide functionalized graphene oxide. Chem Eng J 332:340–350
10. Li ZJ, Wang L, Yuan LY et al (2015) Efficient removal of uranium from aqueous solution by zero-valent iron nanoparticle and its graphene composite. J Hazard Mater 290:26–33
11. Sun YB, Ding CC, Cheng WC et al (2014) Simultaneous adsorption and reduction of U(VI) on reduced graphene oxide-supported nanoscale zerovalent iron. J Hazard Mater 280:399–408
12. Fan FL, Qin Z, Bai J et al (2012) Rapid removal of uranium from aqueous solutions using magnetic Fe_3O_4@SiO_2 composite particles. J Environ Radioact 106:40–46
13. Zhao Y, Li J, Zhao L et al (2014) Synthesis of amidoxime-functionalized Fe_3O_4@SiO_2 core-shell magnetic microspheres for highly efficient sorption of U(VI). Chem Eng J 235:275–283
14. Tan L, Zhang X, Liu Q et al (2015) Synthesis of Fe_3O_4-TiO_2 core-shell magnetic composites for highly efficient sorption of uranium (VI). Colloids Surf A Physicochem Eng Asp 469:279–286
15. Zhang J, Guo Z, Li Y et al (2016) Effect of environmental conditions on the sorption of uranium on Fe_3O_4@MnO_2 hollow spheres. J Mol Liq 223:534–540
16. Loukanov A, Udono H, Takakura R et al (2017) Monitoring and extraction of uranium in polluted acid mine drainage by super-paramagnetic nanoparticles coated with carbon nanodots. J Radioanal Nucl Chem 314(2):1149–1159
17. El-Sherif RM, Lasheen TA, Jebril EA (2017) Fabrication and characterization of CeO_2-TiO_2-Fe_2O_3 magnetic nanoparticles for rapid removal of uranium ions from industrial waste solutions. J Mol Liq 241:260–269
18. Xu M, Han X, Hua D (2017) Polyoxime-functionalized magnetic nanoparticles for uranium adsorption with high selectivity over vanadium. J Mater Chem A 5:12278–12284
19. Han R, Zou W, Wang Y et al (2007) Removal of uranium(VI) from aqueous solutions by manganese oxide coated zeolite: discussion of adsorption isotherms and pH effect. J Environ Radioact 93(3):127–143
20. Yaroshenko NA, Perlova OV, Sazonova VF et al (2012) Sorption of uranium compounds by zirconium-silica nanosorbents. Russ J Appl Chem 85(6):849–855
21. Perlova OV, Sazonova VF, Yaroshenko NA et al (2014) Kinetics of sorption of uranium (VI) compounds with zirconium-silica nanosorbents. Russ J Phys Chem A 88(6):1012–1016
22. Yang D, Song S, Zou Y et al (2017) Rational design and synthesis of monodispersed hierarchical SiO_2@layered double hydroxide nanocomposites for efficient removal of pollutants from aqueous solution. Chem Eng J 323:143–152
23. Zou Y, Wang P, Yao W et al (2017) Synergistic immobilization of UO_2^{2+} by novel graphitic carbon nitride@layered double hydroxide nanocomposites from wastewater. Chem Eng J 330:573–584
24. Cakir P, Inan S, Altas Y (2014) Investigation of strontium and uranium sorption onto zirconium-antimony oxide/polyacrylonitrile (Zr-Sb oxide/PAN) composite using experimental design. J Hazard Mater 271(3):108–119
25. Yuan D, Chen L, Xiong X et al (2016) Removal of uranium (VI) from aqueous solution by amidoxime functionalized superparamagnetic polymer microspheres prepared by a controlled radical polymerization in the presence of DPE. Chem Eng J 285:358–362
26. Yu HW, Yang SS, Ruan HM et al (2015) Recovery of uranium ions from simulated seawater with palygorskite/amidoxime polyacrylonitrile composite. Appl Clay Sci 111:67–75
27. Bai J, Yin X, Zhu Y et al (2016) Selective uranium sorption from salt lake brines by amidoximated Saccharomyces cerevisiae. Chem Eng J 283:889–895
28. Shen L, Han X, Qian J et al (2017) Amidoximated poly(vinyl imidazole)-functionalized molybdenum disulfide sheets for efficient sorption of a uranyl tricarbonate complex from aqueous solutions. RSC Adv 7:10791–10797

29. Liu Y, Li Q, Cao X et al (2013) Removal of uranium(VI) from aqueous solutions by CMK-3 and its polymer composite. Appl Surf Sci 285:258–266
30. Shao D, Hou G, Li J et al (2014) PANI/GO as a super adsorbent for the selective adsorption of uranium (VI). Chem Eng J 255:604–612
31. Turanov AN, Karandashev VK, Masalov VM et al (2013) Adsorption of lanthanides(III), uranium(VI) and thorium(IV) from nitric acid solutions by carbon inverse opals modified with tetraphenylmethylenediphospine dioxide. J Colloid Interface Sci 405:183–188
32. Abdeen Z, Akl ZF (2015) Uranium (VI) adsorption from aqueous solutions using poly(vinyl alcohol)/carbon nanotube composites. RSC Adv 5:74220–74229
33. Al Keshtkar AR, Irani M, Moosavian A (2013) Removal of uranium (VI) from aqueous solutions by adsorption using a novel electrospun PVA/TEOS/APTES hybrid nanofiber membrane: comparison with casting PVA/TEOS/APTES hybrid membrane. J Radioanal Nucl Chem 295(1):563–571
34. Rahmani-Sani A, Hosseini-Bandegharaei A, Hosseinib S-H et al (2015) Kinetic, equilibrium and thermodynamic studies on sorption of uranium and thorium from aqueous solutions by a selective impregnated resin containing carminic acid. J Hazard Mater 286:152–163
35. Elabd AA, Zidan WI, Abo-Aly MM et al (2014) Uranyl ions adsorption by novel metal hydroxides loaded Amberlite IR 120. J Environ Radioact 134:99–108
36. Zidan WI, Abo-Aly MM, Elhefnawy OA et al (2014) Batch and column studies on uranium adsorption by Amberlite XAD-4 modified with nano-manganese dioxide. J Radioanal Nucl Chem 304(2):645–653
37. Dzyazko YS, Perlova OV, Perlova NA et al (2017) Composite cation-exchange resins containing zirconium hydrophosphate for purification of water from U(VI) cations. Desalin Water Treat 69:142–152
38. Perlova N, Dzyazko Y, Perlova O et al (2017) Formation of zirconium hydrophosphate nanoparticles and their effect on sorption of uranyl cations. Nanoscale Res Lett 12:209. https://doi.org/10.1186/s11671-017-1987-y
39. Gao Q, Hu J, Li R et al (2016) Radiation synthesis of a new amidoximated UHMWPE fibrous adsorbent with high adsorption selectivity for uranium over vanadium in simulated seawater. Radiat Phys Chem 122:1–8
40. Zhang S, Zhao X, Li B et al (2016) "Stereoscopic" 2D super-microporous phosphazene-based covalent organic framework: design, synthesis and selective sorption towards uranium at high acidic condition. J Hazard Mater 314:95–104
41. Heshmati H, Torab-Mostaedi M, Gilani HG et al (2015) Kinetic, isotherm, and thermodynamic investigations of uranium(VI) adsorption on synthesized ion-exchange chelating resin and prediction with an artificial neural network. Desalin Water Treat 55(4):1076–1087
42. Zhou L, Zou H, Huang Z et al (2016) Adsorption of uranium (VI) from aqueous solution using magnetic carboxymethyl chitosan nano-particles functionalized with ethylenediamine. J Radioanal Nucl Chem 308(3):935–946
43. Şimşek S, Yilmaz E, Boztuğ A (2013) Amine-modified maleic anhydride containing terpolymers for the adsorption of uranyl ion in aqueous solutions. J Radioanal Nucl Chem 298 (2):923–930
44. Su S, Liu Q, Liu J et al (2017) Enhancing adsorption of U(VI) onto EDTA modified L. cylindrica using epichlorohydrin and ethylenediamine as a bridge. Sci Rep 7:44156. https://doi.org/10.1038/srep44156
45. Dzyazko YS, Ponomareva LN, Volfkovich YM et al (2012) Effect of the porous structure of polymer on the kinetics of Ni^{2+} exchange on hybrid inorganic-organic ionites. Russ J Phys Chem 86(6):913–919
46. Dzyazko YS, Ponomaryova LN, Volfkovich YM et al (2014) Ion-exchange resin modified with aggregated nanoparticles of zirconium hydrophosphate. Morphology and functional properties. Microporous Mesoporous Mater 198:55–62
47. Myronchuk VG, Dzyazko YS, Zmievskii YG et al (2016) Organic-inorganic membranes for filtration of corn distillery. Acta Periodica Technologica 47:153–165

48. Dzyazko YS, Volfkovich YM, Ponomaryova LN et al (2016) Composite ion-exchangers based on flexible resin containing zirconium hydrophosphate for electromembrane separation. J Nanosci Technol 2(1):43–49
49. Cormelis R, Caruso JA, Crews H et al (2005) Handbook of elemental speciation II. Species in the environment, food, medicine and occupational health. Wiley, Chichester
50. Amphlett CB (1964) Inorganic ion exchangers. Elsevier, Amsterdam
51. Dzyazko YS, Rozhdestvenskaya LM, Vasilyuk SL et al (2009) Electrodeionization of Cr(VI)-containing solution. Part I: chromium transport through granulated inorganic ion-exchanger. Chem Eng Commun 196(1–2):3–21
52. Maltseva TV, Kudelko EO, Belyakov VN (2009) Adsorption of Cu(II), Cd(II), Pb(II), Cr(VI) by double hydroxides on the basis of Al oxide and Zr, Sn, and Ti oxides. Russ J Phys Chem A 83 (13):2336–2339
53. Dzyaz'ko YS, Belyakov VN, Vasilyuk SL et al (2006) Anion-exchange properties of composite ceramic membranes containing hydrated zirconium dioxide. Russ J Appl Chem 79(5):769–773
54. Dzyazko YS, Volfkovich YM, Sosenkin VE et al (2014) Composite inorganic membranes containing nanoparticles of hydrated zirconium dioxide for electrodialytic separation. Nanoscale Res Lett 9:271. https://doi.org/10.1186/1556-276X-9-271
55. Marti-Calatayud MC, Garcia-Gabaldon M, Perez-Herranz V et al (2015) Ceramic anion-exchange membranes based on microporous supports infiltrated with hydrated zirconium dioxide. RSC Adv 5:46348–46358
56. Dzyazko YS, Rudenko AS, Yukhin YM et al (2014) Modification of ceramic membranes with inorganic sorbents. Application to electrodialytic recovery of Cr(VI) anions from multicomponent solution. Desalination 342:52–60
57. Pang R, Li X, Li J et al (2014) Preparation and characterization of ZrO_2/PES hybrid ultrafiltration membrane with uniform ZrO_2 nanoparticles. Desalination 332:60–66
58. Dzyazko YS, Rozhdestvenska LM, Vasilyuk SL et al (2017) Composite membranes containing nanoparticles of inorganic ion exchangers for electrodialytic desalination of glycerol. Nanoscale Res Lett 12:438. https://doi.org/10.1186/s11671-017-2208-4
59. Mal'tseva TV, Kolomiets EA, Vasilyuk SL (2017) Hybrid adsorbents based on hydrated oxides of Zr(IV), Ti(IV), Sn(IV), and Fe(III) for arsenic removal. J Water Chem Technol 39(4):214–219
60. Kolomiets EA, Belyakov VN, Palchik AV et al (2017) Adsorption of arsenic by hybrid anion–exchanger based on titanium oxyhydrate. J Water Chem Technol 39(2):80–84
61. Savvin SB (1961) Analytical use of arsenazo III: determination of thorium, zirconium, uranium and rare earth elements. Talanta 8:673–685
62. Myerson AS (ed) (2002) Handbook of industrial crystallization. Butterworth-Heinemann, Woburn
63. Ostwald WF (1888) Zur Theorie der Lösungen. Z Phys Chem 2(1):36–37
64. Dzyazko YS, Ponomareva LN, Volfkovich YM et al (2013) Conducting properties of a gel ionite modified with zirconium hydrophosphate nanoparticles. Russ J Electrochem 49(3):209–215
65. Kostrikin AV, Spiridonov FM, Komissarova LN (2010) On the structure and dehydration of hydrous zirconia and hafnia xerogels. Russ J Inorg Chem 55(6):866–875
66. Helfferich F (1995) Ion exchange. Dover, New York
67. Lagergren S (1898) About the theory of so called adsorption of soluble substances. Kungliga Svenska Vetenskapsakademiens Handlingar 24(4):1–39
68. Ho YS, McKay G (1999) Pseudo-second order model for sorption processes. Process Biochem 34(5):451–465